Ab initio study of the mechanisms of intermolecular and intramolecular [4 + 2] cycloaddition reactions of conjugated enynes

ARTICLE *in* JOURNAL OF PHYSICAL ORGANIC CHEMISTRY · FEBRUARY 2001

Impact Factor: 1.38 · DOI: 10.1002/1099-1395(200102)14:2<109::AID-POC344>3.0.CO;2-J

1 AUTHOR:

Valentine P. Ananikov
Russian Academy of Sciences
141 PUBLICATIONS **2,900** CITATIONS

JOURNAL OF PHYSICAL ORGANIC CHEMISTRY
J. Phys. Org. Chem. 2001; **14:** 109–121

Ab initio study of the mechanisms of intermolecular and intramolecular [4 + 2] cycloaddition reactions of conjugated enynes

Valentine P. Ananikov*

N. D. Zelinsky Institute of Organic Chemistry, Russian Academy of Sciences, Leninsky Prospect 47, Moscow 117913, Russia

Received 10 July 2000; revised 2 November 2000; accepted 3 November 2000

epoc ABSTRACT: The mechanisms of intermolecular and intramolecular enyne [4 + 2] cycloaddition reactions were investigated in detail using high-level *ab initio* methods. The structures of all transition states and intermediates were located using the MP2 method, potential energy surfaces were calculated at the MP2, MP3, MP4(SDQ), MP4(SDTQ), CCSD and CCSD(T) theory levels and the solvent effect was studied within PCM model. Copyright © 2001 John Wiley & Sons, Ltd.
Additional material for this paper is available from the epoc website at http://www.wiley.com/epoc

KEYWORDS: cycloaddition reaction; hydrogen shift; MP2; MP3; MP4(SDTQ); CCSD(T); polarization continuum model

INTRODUCTION

Recently, a wide class of [4 + 2] cycloaddition reactions was enriched with a new example, where enynes and diynes may be used as four-electron donors[1–3]. The simplest reactions of this type are depicted in Scheme **1**. Intermolecular reaction was not recognized as a valuable synthetic method whereas in contrast, intramolecular [4 + 2] enyne cycloaddition (Scheme **1**) has found substantial application in experimental synthesis as an efficient and general route for ring construction of aromatic and dihydroaromatic compounds. Various substituted enynes were shown to undergo intramolecular cycloaddition reactions providing a new pathway to bicyclic products.[1–4]

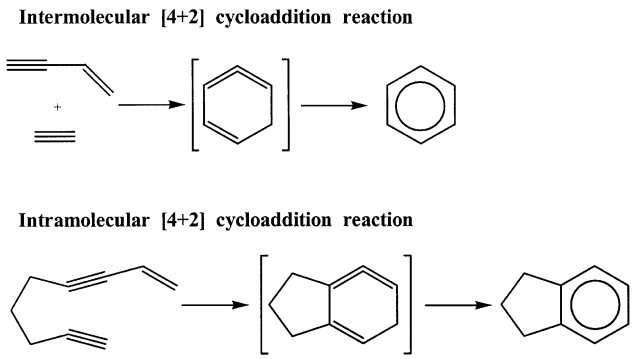

Scheme 1. Inter- and intramolecular [4 + 2] cycloaddition reactions

The proposed mechanism of the reaction is interesting. The six-membered allene (1,2,4-cyclohexatriene and its derivatives) were suggested as reaction intermediates (Scheme **1**). The formation of such species was shown experimentally using various trapping techniques.[5–8] However, six-membered ring allenes have never been isolated or directly observed, which is usually explained on the basis of a large predicted strain energy (see review[6]). An experimental enthalpy of formation of $\Delta_f H°$ = 105.1 kcal mol^{-1} (1 kcal = 4.184 kJ) for 1,2,4-cyclohexatriene has been reported,[9] compared with 19.81 kcal mol^{-1} for benzene,[9] one may assume the compound to be only a highly reactive intermediate.

The electronic structure and stability of 1,2,4-cyclohexatriene are of much interest and have been studied with different theoretical methods. AM1 semiempirical calculations[7] result in $\Delta_f H°$ = 93.7 kcal mol^{-1} (22.0 kcal mol^{-1} for benzene), and recent *ab initio* investigations at the G2(MP2) level[10] report a similar value of $\Delta_f H°$ = 96.2 kcal mol^{-1} (21.1 kcal mol^{-1} for benzene). In both cases the energy is considerably higher than that of benzene, in agreement with the experimental estimation discussed above. The energetic plausibility of cycloaddition reactions leading to allene intermediates was investigated at the MP4//MP2 level of theory,[2] and particularly for 1,2,4-cyclohexatriene the reaction was found to be exothermic, $\Delta G = -13.4$ kcal mol^{-1}; this value is half that -29.7 kcal mol^{-1}, estimated earlier.[1]

**Correspondence to:* V. P. Ananikov, N. D. Zelinsky Institute of Organic Chemistry, Russian Academy of Sciences, Leninsky Prospect 47, Moscow 117913, Russia.
E-mail: val@cacr.ioc.ac.ru

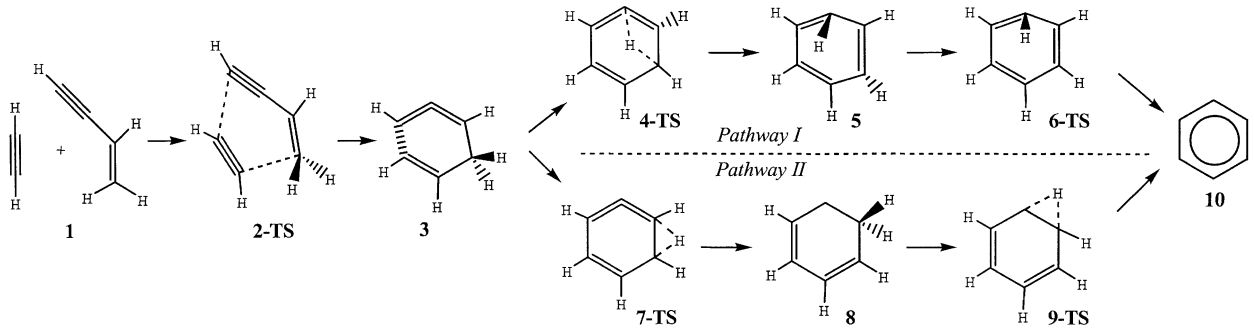

Scheme 2. Mechanism of intermolecular [4 + 2] cycloaddition reaction

An activation barrier of $\Delta G^{\neq} = 42.0$ kcal mol^{-1} for allene formation has also been reported.[2] Much interest in 1,2,4-cyclohexatriene has been shown in theoretical studies devoted to benzene isomers and related isomerization processes[11,12].

Although some partial data on stability and formation of ring-allene intermediates is available, to the best of our knowledge neither transition state structures nor the reaction mechanism of enyne to aromatic system conversion have been reported at the *ab initio* level for both intermolecular and intramolecular [4 + 2] cycloaddition reactions.

Here we present the first detailed *ab initio* study of the mechanism of both intra- and intermolecular [4 + 2] enyne cycloaddition reactions including two alternative ring allene isomerization pathways in each case. ΔG potential energy surfaces of the reactions are presented and discussed in the light of available experimental data. All reactants and transition states were optimized at the MP2 level of theory and energy evaluation with high-level electron correlation methods up to MP4(SDTQ) and CCSD(T) was performed. The solvent effect was investigated using the polarization continuum model (PCM). The potential energy surfaces of both reactions were traced with IRC calculations.

CALCULATION PROCEDURE

The geometries of all reactants, intermediates, transition states and products were optimized using the second-order Møller–Plesset(MP2) method.[13,14] Standard 6–31G* and 6–311++G** basis sets were used throughout[15,16]. Normal coordinate analysis was performed for all stationary points to verify the transition states (one imaginary frequency) and equilibrium structures (no imaginary frequencies) and to calculate the zero-point energy correction and Gibbs free energy. The latter values were used to construct ΔG potential energy surfaces. All transition states were confirmed with forward and backward IRC calculations.[17]

The solvent effect was studied with the PCM method.[18–20] The MP2/6–31G* optimized geometry was used to run single-point PCM calculations, since it has been shown that the free energy hypersurfaces in solution are very flat and reoptimization has a very limited effect.[21] This approach has been tested in numerous cases and provides a reliable description of the solvent effect.[18–20] For a set of neutral molecules, which includes some of the reactants and products of the intermolecular reaction studied here, the mean error with respect to experimental solvation energy was found to be <0.2 kcal mol^{-1}.[21] To determine the relative free energies in solution for the studied potential energy surfaces, the relative free energies of solvation were added to the relative free energies in the gas phase.

To estimate the accuracy of geometry optimization, MP2/6–31G* optimized structures of the initial reactants and products of the intermolecular reaction were compared with available literature data.[22] The comparison revealed mean deviations about 0.01 Å and 1° for bond lengths and bond angles, respectively, thus confirming an adequate geometry description.

High-level electron correlation methods, such as MP3, MP4(SDQ), MP4(SDTQ),[23,40,41] CCSD and CCSD(T)[28–31] were applied to the MP2 optimized geometry.

All MP2, MP3, MP4(SDQ) and MP4(SDTQ) calculations were performed using the PC-GAMESS version[32] of the GAMESS/US program.[33] The calculations were carried out on a laboratory-made Intel CPU-based Linux cluster. UMP2, PCM, CCSD and CCSD(T) calculations were performed with the Gaussian 98[34] package. MOLDEN was used for molecular graphics visualization.[35]

RESULTS

Intermolecular [4 + 2] cycloaddition reaction of conjugated enyne and acetylene

In this section the potential energy surface of the [4 + 2] cycloaddition reaction is described. Two alternative pathways of allene isomerization are considered in detail.

The detailed reaction scheme is shown on Scheme **2** and optimized structures and geometry parameters are given in Fig. 1. Energy data are summarized later in

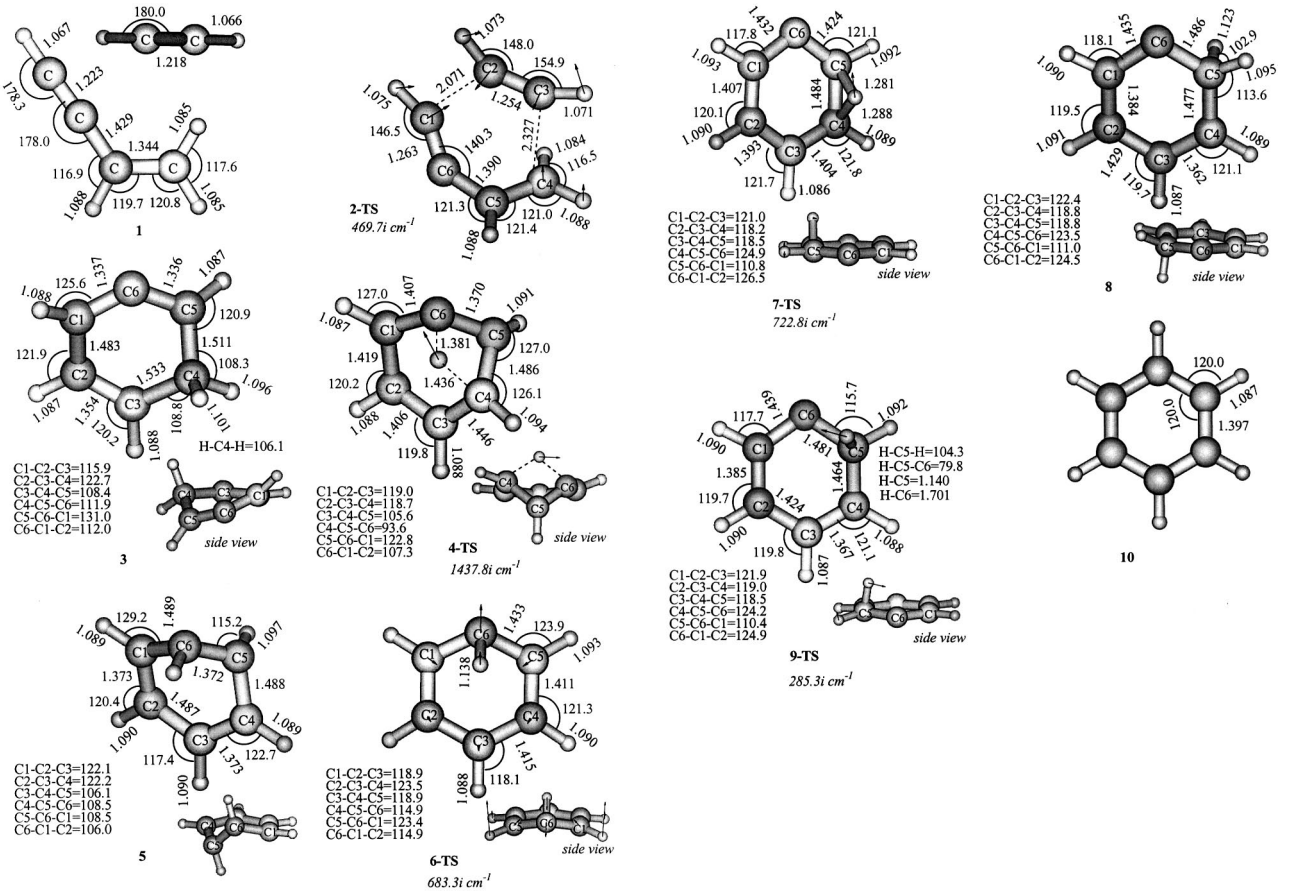

Figure 1. MP2 optimized structures of initial compounds, transition states, intermediates and products of intermolecular reaction. Displacement vectors corresponding to imaginary frequency are shown for each transition state

Table 1. The ΔG potential energy surface is presented on PES 1 A (see Fig. 3).

The mechanism of the reaction will be considered using the ΔG potential energy surface as the most reliable one. A separate discussion of the energy and ZPVE corrected energy surfaces will be given in the Discussion section.

The cycloaddition step. The [4 + 2] cycloaddition reaction of enyne and acetylene takes place through the transition state **2-TS**. Normal-mode analysis shows that the structure has only one imaginary frequency of 469.7*i* cm^{-1}; IRC calculations were carried out to confirm that **2-TS** really connects reactants **1** to product **3**. Both acetylene and enyne geometries significantly perturb upon the transition state formation. The carbon–carbon triple bonds become longer by about 0.04 Å, while the length of the double bond increases by 0.03 Å. The acetylene unit is no longer linear in the transition state, the H—C—C bond angle decreases from 180° to 148.0° and to 154.9° for H—C_2—C_3 and H—C_3—C_2, respectively. The same trends are observed in the enyne fragment, where the H—C_1—C_6 and C_1—C_6—C_5 bond angles deviate from a linear form by 33.5° and 39.7°, respectively. It should be noted also that carbon–carbon bond formation between sp-hybridized atoms requires a much shorter distance in the transition state than between sp–sp^2 carbon atoms, C_1—C_2 = 2.071 Å and C_3—C_4 = 2.327 Å.

Transition state **2-TS** leads to the non-planar six-membered ring allene **3**. The molecule contains two 1,2-cumulene double bonds with very close lengths, C_1—C_6 = 1.337 Å and C_5-C_6 = 1.336 Å and an additional double bond is formed between carbon atoms C_2 and C_3. The changes in C—H bond lengths compared with the initial compounds **1** are in good agreement with the expected values since all atoms, except C_3, adopt a new hybridization.

The geometry of the C═C═C unit in non-cyclic allenes is in most cases linear, whereas in the six-membered ring **3** the C_5—C_6—C_1 angle is 131.0°. This leads to a significant increase in strain energy and is believed to be the main cyclic allene instability factor.

To reach transition state **2-TS** an activation energy of 39.2 kcal mol^{-1} is required; the reaction is exothermic by 13.2 kcal mol^{-1}.

Allene isomerization through Pathway I. Experimen-

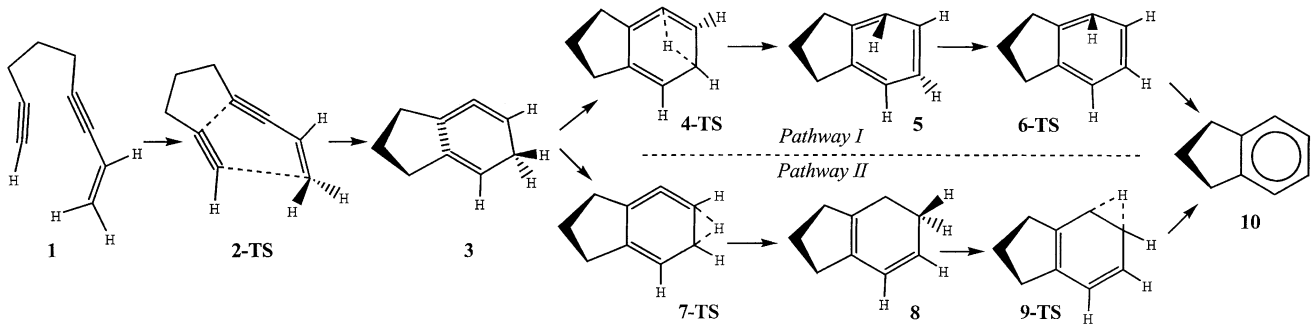

Scheme 3. Mechanism of intramolecular [4 + 2] cycloaddition reaction

tal studies indicated an aromatic system as the final product of the cycloaddition reaction. The easiest way to form the benzene **10** from the allene **3** can be a $C_4 \rightarrow C_6$ hydrogen shift as denoted in Scheme **2**. The corresponding transition state **4-TS** has been located and the imaginary mode of 1437.8i cm^{-1} represents the hydrogen shift reaction path. An activation energy of 45.6 kcal mol^{-1} is needed to reach the transition state. The high activation energy reflects increased strain in **4-TS**, since the C_4—C_5—C_6 bond angle has to be reduced to 93.6° compared with 111.9° in **3**. The reaction is endothermic by 20.3 kcal mol^{-1} and, in agreement with the Hammond postulate, the transition state has more product-like character: the breaking C—H bond is significantly longer than the forming bond, C_4—H = 1.436 Å and C_6—H = 1.381 Å.

Surprisingly, forward IRC calculations lead to *cis, cis, trans*-1,3,5-cyclohexatriene **5**, rather than benzene, as a final product of this step. Compound **5** is not planar and the necessary conditions for aromatic electron delocalization cannot be met. According to the geometry parameters in **5** the six-membered ring is formed from three single and three double carbon–carbon bonds with lengths in the range 1.487–1.489 and 1.372–1.373 Å, respectively. *cis, cis, trans*-1,3,5-cyclohexatriene **5** is a subject of much attention in view of its possible existence and after electronic structure elucidation it was finally referred as a 'Möbius benzene'.[36]

The MP2 optimized geometry of **5** is shown in Fig. 1 and it agrees very well with available literature predictions[36] for 'Möbius benzene'. The non-planar benzene isomer may form an aromatic system through the transition state **6-TS;** normal-mode analysis gives one imaginary frequency of 683.3*i* cm^{-1}. The IRC calculations confirm this isomerization step. An activation energy of 21.2 kcal mol^{-1} is required to form the transition state **6-TS** and the step is exothermic by 103.4 kcal mol^{-1} relative to **5**. Such a large exothermicity is not surprising since a conjugated aromatic system is formed from the highly strained precursor.

There is some experimental evidence that such *trans*-to *cis* isomerization may proceed through a diradical-type transition state. Surprisingly, while trying to calculate the single–triplet gap, it was found that attempts to UMP2/6–31G* optimization of a triplet state of **5** starting from different initial geometries led to spontaneous isomerization of the *trans* double bond. Such behavior of the system is in excellent agreement with the predicted very shallow minima for 'Möbius benzene', which may interconvert to benzene with an extremely low barrier of $\Delta G^{\neq}$ = 0.9 kcal mol^{-1} calculated at the CASSCF(6,6)/6–31G*//CASSCF(6,6)/3–21G level.[36] We recalculated the activation barrier at the CASSCF(6,6)/3–31G*//CASSCF(6,6)/6–31G* level and found a value of only $\Delta G^{\neq}$ = 1.5 kcal mol^{-1}. Dihedral H—C_1—C_2—H angles in 'Möbius benzene' and the conversion transition state are 179.2° and 150.6°, respectively; optimized at the CASSCF(6,6)/6–31G* level, the angle finally decreases to zero in benzene. An early character of the transition state agrees with a relatively small barrier height. Therefore, the energy minimum for **5** is really very shallow and can be easily overcome during geometry optimization, especially taking into account the high exothermicity of the process. The results indicate that isomerization of *cis, cis, trans*-1,3,5-cyclohexatriene **5** may take place through a diradical mechanism rather than through the singlet state **6-TS**. The activation barrier at the CASSCF(6,6)/6–31G* level is very small and the barrier is negligible at the UMP2/6–31G* level of theory, so it was not possible to obtain transition state structures at the latter case.

Finally, the rate-determining stage of the Pathway I is the first 1,3-hydrogen shift leading to *cis, cis, trans*−1,3,5-cyclohexatriene, which may interconvert to benzene without a noticeable activation barrier.

Allene isomerization through Pathway II. The alternative pathway to form benzene from the cyclic allene **3** may proceed via two subsequent 1,2-hydrogen shifts instead of a single 1,3-shift described above. Starting from allene **3** a $C_4 \rightarrow C_5$ hydrogen shift occurs through the transition state **7-TS** with an activation energy of 31.1. kcal mol^{-1}. The point on the reaction path which corresponds to the product **8** lies 16.3 kcal mol^{-1} higher compared with reactant **3**. The hydrogen shift transition state has a three-membered structure with very similar

C_4—H and C_5—H bond lengths, 1.288 and 1.281 Å, respectively. The calculations show that a relatively small activation energy is required to break the allene system and to isomerize double bonds. The final product of this step, compound **8**, contains two double and four single carbon–carbon bonds and a carbene center on the former allene center at C_6. The compound is 4.0 kcal mol^{-1} more stable than 'Möbius benzene' **5** (see Pathway I). According to previous experimental and theoretical investigations, intramolecular rearrangements in carbenes proceed via the singlest state[11,12,37–39] and therefore the further mechanistic considerations are restricted to the singlest state of **8**.

The second $C_5 \rightarrow C_6$ hydrogen shift takes place via transition state **9-TS** with an imaginary frequency of 285.3*i* cm^{-1} almost without a barrier (precise relative MP2 energies on the surface are E(**8**) = −14.230 kcal mol^{-1} and E(**9-TS**) = −14.151 kcal mol^{-1}, giving a barrier of only 0.079 kcal mol^{-1}, which vanishes on the free energy surface). The very small barrier reflects internal instability of the parent compound **8**. Consistent with the large exothermicity of this step (99.4 kcal mol^{-1}) the transition state has a very early character, C_5—H = 1.140 Å, C_6—H = 79.8°. Benzene is found as a final product of the second hydrogen shift. A series of IRC calculations through the transition states **7-TS** and **9-TS** were performed to confirm the Pathway II from allene **3** to the reaction final product **10**.

As in the previously examined pathway, the rate-determining stage is the first hydrogen shift process, which, similarly, leads to a very unstable intermediate compound followed by its final interconversion to benzene almost without a barrier.

Intramolecular [4 + 2] cycloaddition reaction

The potential energy surface of the intramolecular [4 + 2] cycloaddition reaction with both allene isomerization pathways is described in this section. The process represents a real chemical system with no simplifying approximations. Geometry and energy changes outlined for the model intermolecular reaction (see the previous section) will not be repeated here; the main attention will be paid instead to the differences between intermolecular and intramolecular reactions.

The detailed reaction scheme is shown in Scheme **3** and optimized structures and geometry parameters are given on Fig. 2. Energy data are summarized later in Table 3. The ΔG potential energy surface is presented on PES 1B (see Fig. 3).

Again the mechanism of the reaction will be considered using the ΔG potential energy surface and a separate discussion of the energy and ZPVE corrected energy surfaces will be given later.

The cycloaddition step. The intramolecular cycloaddition reaction starts from compound **1** (Fig. 2) in which acetylene and enyne units are connected to each other via the bridging —$(CH_2)_3$— fragment. The molecule may adopt different conformations due to rotation around the carbon–carbon bonds; the appropriate conformation was found using backward IRC calculations from cycloaddition transition state **2-TS**. The geometry parameters of acetylene and enyne units are very close to those observed in the free molecules (cf. Fig. 1); the units are connected via four C—C bonds with slightly different lengths: C_{SP^3}—C_{SP}=1.462–1.466 Å and C_{SP^3}—C_{SP^3} = 1.535–1.536 Å.

The cycloaddition reaction takes place through the transition state **2-TS**; normal-mode analysis shows one imaginary frequency of 399.8*i* cm^{-1}. An activation energy of 27.9 kcal mol^{-1} is required to reach **2-TS**, which is 11.3 kcal mol^{-1} lower than the model intermolecular reaction result. In agreement with the tendencies mentioned earlier, all unsaturated C—C bonds become longer in the transition state and the bond angles decrease significantly. The changes in **2-TS** geometry concern also methylene groups, where the smallest bond angle decrease is found for C_4—C_5—C_6, Δ = 5.5°, and the largest for C_5—C_6—C_7, Δ = 36.8°. In contrast to the intermolecular model reaction, C—C bond information in the intramolecular transition state takes place with much smaller difference in distances C_4—C_8 = 2.127 Å and C_1—C_9 = 2.175 Å (cf. C_1—C_2 = 2.017 Å and C_3—C_4 = 2.327 Å. Fig. 1).

Transition state **2-TS** leads to the bicyclic compound **3**. The larger ring is a six-membered ring allene, the same as formed in the model intermolecular reaction; the five-membered ring contains all the bridging methylene groups. The cycloaddition reaction is exothermic by 14.2 kcal mol^{-1}. According to the IRC calculations, both rings in **3** have non-planar conformations (see side view).

Allene isomerization through Pathway I. A 1,3-hydrogen shift (from C_1 to C_3) takes place through the transition state **4-TS** and the imaginary mode of 1451.8*i* cm^{-1} represents the reaction path. The presence of the second ring does not introduce significant changes into the structure of the transition state, hence the activation energy is almost unaffected, $\Delta G^{\neq}$ = 45.1 kcal mol^{-1} (cf. $\Delta G^{\neq}$ = 45.6 kcal mol^{-1} for the intermolecular process). Again, forward IRC calculations from **4-TS** do not lead to the aromatic system as a final product of ring allene isomerization via the 1,3-hydrogen shift. A substituted 'Möbius benzene' structure with a trans C_1=C_2 double bond is formed instead. The formation of **5** from **3** is endothermic by 16.5 kcal mol^{-1}, the appropriate value from the model intermolecular process is 20.3 kcal mol^{-1}, suggesting some stabilization from the five-membered ring.

The last isomerization step of Pathway I proceeds through **6-TS** and requires 21.1 kcal mol^{-1} activation

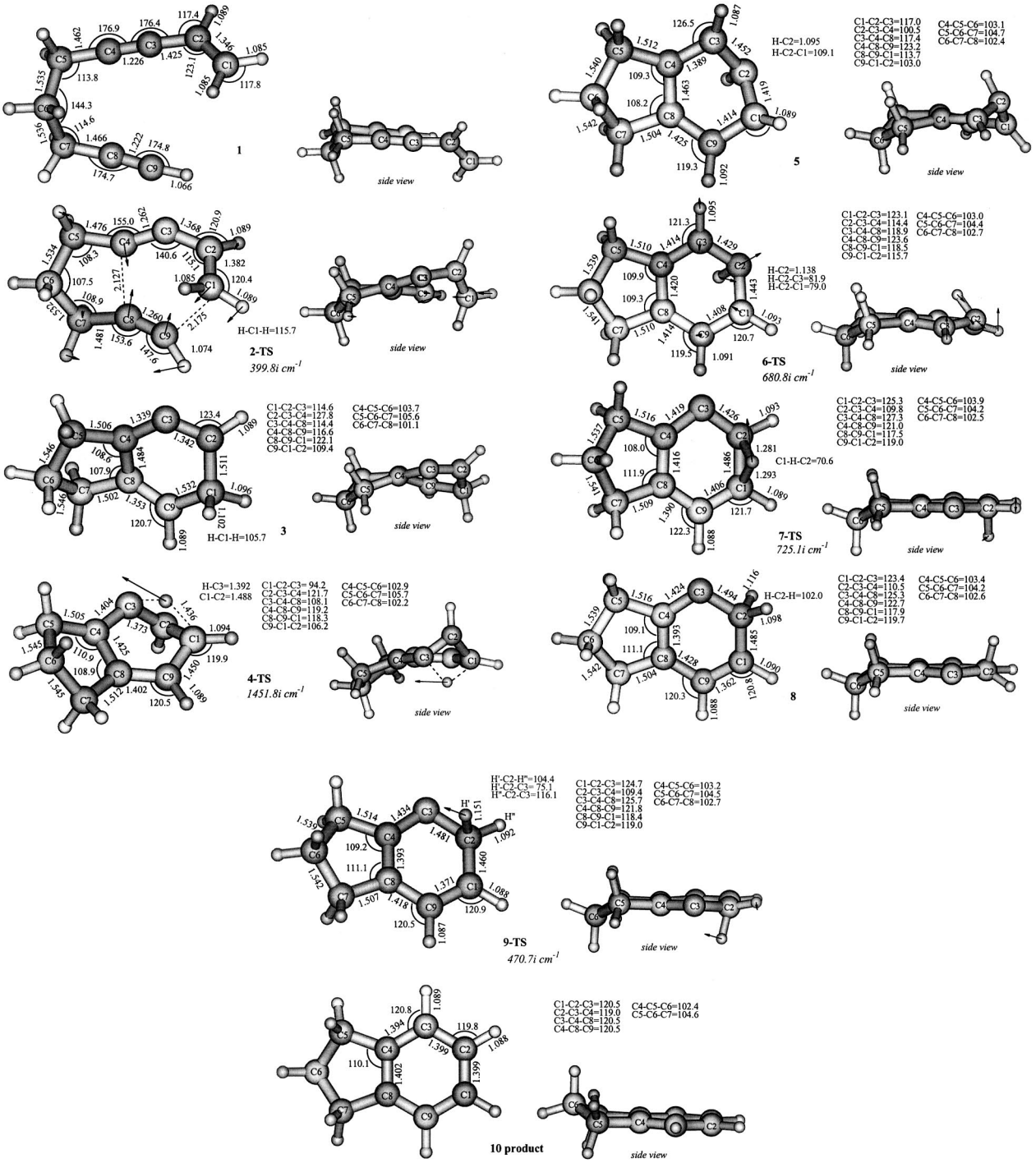

Figure 2. MP2 optimized structures of initial compounds, transition states, intermediates and products of intramolecular reaction. Displacement vectors corresponding to imaginary frequency are shown for each transition state

energy (cf. 21.2 kcal mol^{-1} for the intermolecular process). Aromatic system formation is exothermic by 101.3 kcal mol^{-1} compared with **5** and by 99.0 kcal mol^{-1} compared with the initial compound **1**. The IRC calculations were run to confirm the nature of transition states **4-TS** and **6-TS**.

Applying UMP2/6–31G* calculations to the triplet state of **5** initiates spontaneous isomerization, as was already found for the intermolecular reaction, thus showing very shallow minima for **5**.

Allene isomerization through Pathway II. In contrast to isomerization Pathway I, where the activation barriers are almost unaffected, addition of the second ring significantly lowers the barrier of the 1,2-hydrogen shift of Pathway II, $\Delta G^{\neq} = 26.1$ kcal mol^{-1} (cf. $\Delta G^{\neq} = 31.1$

Table 1. Relative energy at different theory levels, ZPVE corrected energy and Gibbs free energy ΔG at the MP2/6–31G*//MP2/6–31G* level of intermolecular acetylene and enyne reaction (in kcal mol[a])

Species	MP2/6–31*// MP2/6–31G*	MP2/6–31G*// MP2/6–31G* +ZPVE	MP2/6–31G*// MP2/6–31G* ΔG	MP2/6–311++G**// MP2/6–311++G**	MP2/6–311++G**// MP2/6–31G*
1	0.0	0.0	0.0	0.0	0.0
2-TS	25.7	28.9	39.2	23.6	23.7
3	−31.6	−24.3	−13.2	−29.8	−29.8
4-TS	16.8	21.1	32.4		13.7
5	−10.3	−3.5	7.1		−10.3
6-TS	10.9	17.1	28.3		6.6
7-TS	1.3	6.7	17.9	−1.9	−1.8
8	−14.2	−7.6	3.1	–	−14.1
9-TS	−14.2	−8.2	2.9		−14.8
10	−116.3	−107.5	−96.3	−112.4	−112.4

[a] Absolute energies for **1** (in a.u.) for the data from the first through the fifth column, respectively: −231.2724194, −231.1857794, −231.2312656, −231.4142781, −231.4142535.

kcal mol^{-1} for the intermolecular process). The step is endothermic by $\Delta G = 10.9$ kcal mol^{-1} (cf. $\Delta G = 16.3$ kcal mol^{-1} for the intermolecular process). Both the activation energy and endothermicity of the first step of Pathway II are significantly reduced compared with intermolecular reaction. However, since geometry parameters do not show significant differences (cf. Figs 1 and 2), one may conclude that the stabilization effect comes mainly from electronic factors.

The second hydrogen shift of the pathway takes place via **9-TS**, for which one imaginary mode of 470.7*i* cm^{-1} was calculated. According to the H^1—C_2—C_3 angle of 75.1°, the transition state of the intermolecular reaction is more product-like compared with the intermolecular model reaction (H^1—C_2—C_3 = 79.8°). In agreement with the Hammond postulate, the activation energy of the former is higher, $\Delta G^{\neq} = 0.7$ kcal mol^{-1}. Obviously, the value is so small that the barrier can be easily overcome under the reaction conditions.

The IRC calculations confirm that the final product **10** and the ring allene **3** really are connected via the transition states **7-TS** and **9-TS**.

Reliability evaluation of the calculations with respect to basis set, high-level electron correlation and solvent effects

Basis set effect study. To check the reliability of the calculation methods employed, the basis set effects were studied in more detail. The question is of particular importance, since the calculations on the model intermolecular reaction are followed by the investigation of a larger intramolecular chemical system, for which a choice of an accurate and computationally adequate method is of vital importance.

Full geometry optimization of the initial compounds, transition states and products for the two most important steps of the intermolecular reaction, namely cycloaddition and first hydrogen shift of pathway II, were performed at the MP2/6–311++G** level. The final energies (Table 1) show very good agreement with the results obtained from MP2/6-31G* calculations. The activation energy of the cycloaddition reaction is 23.6 kcal mol^{-1} and the reaction is exothermic by 29.8kcal mol^{-1}. Comparison with the respective values at the MP2/6–31G* level 25.7 and 31.6 kcal mol^{-1} shows agreement within 10%.

The hydrogen shift through the transition state **7-TS** requires 27.9 and 32.9 kcal mol^{-1} according to MP2/6–311++G** and MP2/6–31G* calculations, respectively. Hence basis set enhancement slightly decreases the barrier. An attempt of reoptimizing compound **8** at the MP2/6–311++G** level led to a spontaneous second hydrogen shift during geometry optimization forming benzene. The energy difference between **8** and **9-TS** is very small at the MP2/6–31G* level (see earlier), hence the rearrangement is not surprising, especially taking into account that basis set enhancement may lower the barrier of the hydrogen shift further.

At the MP2/6–311++G** level, benzene formation is 112.4 kcal mol^{-1} exothermic compared with initial compound **1**, which deviates from the MP2/6–31G* value by <5%.

Single-point MP2/6–311++G** calculations with MP2/6–31G* optimized geometry give energy values which are in total agreement with the MP2/6–311++G** optimized values (maximum deviation 0.1 kcal mol^{-1}. This indicated that the basis set effect on geometry is really very small. MP2/6–311++G**//MP2/6–31G* calculations for the whole reaction potential energy surface were performed (Table 1) and showed good agreement with those at the MP2/6–31G* level. The largest deviation is found for the hydrogen shift reaction, where increasing basis set quality makes the barriers smaller by about 5 kcal mol^{-1}.

Table 2. Relative energies at different correlation energy levels of intermolecular acetylene and enyne reaction (in kcal mol^{-1})[a]

	X/6–31G*//MP2/6–31G*					X/6–311++//MP2/6–31G*		
Species	X = MP3	MP4(SDQ)	MP4(SDTQ)	CCSD	CCSD(T)	MP3	MP4(SDQ)	MP4(SDTQ)
1	0.0	0.0	0.0	0.0	0.0	0.0	0.0	0.0
2-TS	36.0	37.3	28.4	37.3	31.4	35.5	37.4	27.2
3	−34.8	−31.5	−32.8	−31.5	−34.2	−32.2	−28.8	−30.5
4-TS	24.8	27.8	19.8	28.4	22.0	23.7	27.0	17.6
5	−11.6	−8.4	−11.3	−8.3	−12.5	−10.3	−6.9	−10.5
6-TS	13.9	18.0	13.2	17.2	12.9	11.0	15.4	9.8
7-TS	2.2	6.8	3.6	7.6	5.3	−0.2	4.8	1.1
8	−19.7	−16.1	−15.8	−15.6	−16.2	−19.2	−15.5	−15.3
9-TS	−18.6	−14.8	−15.0	−14.3	−15.0	−18.7	−14.7	−15.2
10	−115.9	−110.6	−112.2	−110.6	−111.3	−111.7	−106.1	−107.6

[a]Absolute energies for **1**(in a.u.) for X/6–31G*//MP2/6–31G* calculations: X = MP3, E = −231.3015973; X = MP4(SDQ), *E* = −231.3171007; X = MP4(SDTQ), *E* = −231.3531150; X = CCSD, *E* = −231.3187159; X = CCSD(T), *E* = 231.3533174. For X/6–311++G**//MP2/6–31G* calculations: X = MP3, *E* = −231.4426974; X = MP4(SDQ), *E* = −231.4558446; X = MP4(SDTQ), *E* = −231.5006985.

Finally, it should be noted that the MP2/6–31G* level gives fairly accurate results in geometry and reliable energy for the system studied. The hydrogen shift activation barriers tend to decrease with basis set quality enhancement.

High-level electron correlation calculations. MP2 is well established as an accurate and relatively inexpensive computational method. However, the question of the importance of higher order terms in the perturbation expansion may arise in many cases. The present investigation showed that higher order effects are not negligible. To answer the question quantitatively, MP3, MP4(SDQ) and MP4(SDTQ)[23,40,41] calculations were applied to the MP2 optimized geometry. In addition, a more accurate high-level treatment of electron correlation provided with coupled cluster theory was applied, particularly using the coupled cluster single and double excitation method (CCSD) and the coupled cluster method with single, double and perturbative triple excitations [CCSD(T)].[28–31] The results are presented in Table 2; MP2 data is given in Table 1.

Analysis of the potential energy surfaces presented in Table 2 shows that the MP3, MP4(SDQ) and CCSD energy surfaces are very close to one another. All the activation energies are reproduced within 1 kcal mol^{-1}. An even smaller deviation of ca 0.5 kcal mol^{-1} in reaction energies is found for the **3**→**8** and **3**→**5** steps. Somewhat larger differences of the order of 3–5 kcal mol^{-1} are observed for the **1**→**3** reaction energy and the exothermicity of the entire reaction (**1**→**10**). This indicates that the MP*n* energies appear to have converged with respect to increasing *n*.

All three methods, MP3, MP4(SDQ) and CCSD, dramatically increase the **1**→**2-TS** and **3**→**4-TS** activation barriers 36.0–37.3 and 59.3–59.9 kcal mol^{-1}, respectively) compared with those calculated at the MP2 level (25.7 and 48.4 kcal mol^{-1}, respectively). The same tendency, but on a smaller scale, is found for **3**→**7-TS** and **5**→**6-TS**, 37.0–39.1 and 25.5–26.4 kcal mol^{-1}, respectively, for the former methods, and 32.9 kcal/mol and 21.2 kcal/mol, respectively, for MP2 calculations. The **8**→**9-TS** barrier is small and is influenced only very slightly.

Full fourth-order Møller–Plesset perturbation theory, MP4(SDTQ), and CCSD(T) calculations result in potential energy surfaces which are similar to each other, but differ substantially from those computed at the MP3, MP4(SDQ) and CCSD levels. The comparison indicates that taking into account triplet excitations is important for the system studied. The activation energies at the MP4(SDTQ) and CCSD(T) levels are intermediate between the MP3, MP4(SDQ) and CCSD values, which are higher, and the MP2 data, which are lower. It is generally believed that the MP4(SDTQ) and CCSD(T) levels usually provide more accurate results, and this is probably true in the system studied since both methods lead to the similar potential energy surfaces. Hence these energy surfaces should be the most reliable. MP3, MP4(SDQ) and CCSD calculations may overestimate the activation barriers by 3–10 kcal mol^{-1}, while MP2 may underestimate them by approximately the same range, 3–8 kcal mol^{-1}. The tendency is less obvious in changes in reaction energies, where the maximum deviation does not exceed 5–6 kcal mol^{-1}. It should be mentioned that MP2 better reproduces exothermicity calculated at the MP4(SDTQ) and CCSD(T) levels.

It is well established that to account accurately all of the correlation energy, substantial basis set improvement may be required. In the system under investigation, basis set improvement from 6–31G* to 6–311++G** led to a few kcal mol^{-1} differences for the MP3, MP4(SDQ) and MP4(SDTQ) energy surfaces (Table 2), thus indicating the convergence with respect to the basis set size.

In summary, a detailed comparison of various theory levels confirmed reasonable accuracy of MP2/6-31G* calculations used as a reference in the present investigation. MP4(SDTQ) and CCSD(T) energies seems to be

Table 3. Relative energy at different theory levels, ZPVE corrected energy and Gibbs free energy (ΔG) at the MP2/6–31G* level of intramolecular reaction (inkcal mol)[a]

Species	MP2/6–31G*// MP2/6–31G*	MP2/6–31G*// MP2/6–31G* +ZPVE	MP2/6–31G*// MP2/6–31G* ΔG	MP3/6–31G*// MP2/6–31G*	MP4(SDQ)/6–31G*// MP2/6–31G*	MP4(SDTQ)6–31G*// MP2/6–31G*
1	0.0	0.0	0.0	0.0	0.0	0.0
2-TS	24.3	25.7	27.9	36.0	36.8	27.3
3	−21.2	−17.0	−14.2	−24.4	−20.6	−22.2
4-TS	26.8	27.9	30.9	35.4	38.7	30.1
5	−3.9	−0.4	2.3	−0.8	3.8	−2.1
6-TS	17.6	20.4	23.4	20.6	25.2	20.1
7-TS	7.1	9.1	11.9	7.8	13.2	9.8
8	−8.8	−5.6	−3.3	−14.9	−10.4	−10.2
9-TS	−7.8	−5.4	−2.6	−12.1	−7.2	−7.9
10	−107.4	−102.0	−99.0	−107.3	−101.4	−103.0

[a] Absolute energies for 1 (in a.u) for the data from the first through the sixth column, respectively: −347.6234875, −347.4653915, −347.5012708, −347.6685485, −347.6898963, −347.7431074.

Table 4. Solvent effect on potential free energy surface (ΔG_{Solv}) according to PCM calculations (in kcal mol^{-1})[a]

	Intermolecular reaction, PCM–MP2/6–31G*				Intramolecular reaction, PCM–MP2/6–31G*			
Species	Toluence (ε = 2.4)	$CHCl_3$ (ε = 4.9)	DMSO (ε = 46.7)	Water (ε = 78.4)	Toluene (ε = 2.4)	$CHCl_3$ (ε = 4.9)	DMSO (ε = 46.7)	Water (ε = 78.4)
1	0.0	0.0	0.0	0.0	0.0	0.0	0.0	0.0
2-TS	37.7	37.9	37.6	37.9	25.9	26.2	25.8	26.4
3	−16.1	−16.2	−17.0	−16.7	−17.1	−17.3	−18.0	−17.5
4-TS	29.4	28.9	28.2	27.8	28.2	28.1	27.4	28.0
5	4.8	5.3	4.9	6.4	−0.3	−0.4	−0.9	0.0
6-TS	24.1	23.2	21.7	19.8	19.3	18.4	17.0	15.6
7-TS	12.5	10.7	8.5	4.9	7.0	6.0	4.0	1.7
8	−1.0	−1.6	−3.0	−4.1	−7.2	−7.7	−9.1	−9.9
9-TS	−1.2	−1.7	−3.1	−4.1	−6.4	−6.9	−8.1	−8.9
10	−99.7	−100.1	−101.2	−101.3	−102.1	−102.4	−103.3	−103.1

[a]Absolute energies for **1** (in a.u.) for intermolecular reaction: toluene, −231.2280784, $CHCl_3$, −231.2298792; DMSO, −231.2283811; water, −231.2308194. For intramolecular reaction: toluene, −347.4992628; $CHCl_3$, −347.4999162; DMSO, −347.5000278; water, −347.5025776.

more accurate by 3–8 kcal mol^{-1} depending on the reaction type, and should be used whenever possible from the available computational resources point of view. Owing to significant deviations from the former MP3, MP4(SDQ) and CCSD single-point calculations are less preferred.

Solvent effect study. Solvation may have a crucial effect on reaction mechanisms. Significant changes in solvation energy upon chemical transformations may, in certain cases, dramatically change the potential energy surface of a reaction.[18–20] Of course, this is mostly the case when charged species are involved, while one would not expect a large solvent effect in hydrocarbon cycloaddition reactions, since they are not accompanied by significant charge delocalization.[18–20]

To investigate the solvent effect, PCM calculations were applied for all points of the potential energy surface. According to experimental data, non-catalyzed thermal [4 + 2] enyne cycloaddition reaction is usually carried out in toluene solution.[1,3] The PCM approximation[18–20] was used to model toluene surrounding and, in addition to the former, the calculations for three other common solvents were performed [chloroform, dimethyl sulfoxide (DMSO) and water]. This may allow one not only to simulate exact experimental conditions, but also to estimate effect of the medium on the mechanism of the reaction in more detail and to make some predictions.

The results of PCM calculations applied at the MP2/6–31G* optimized geometry are presented in Table 4; gas-phase data are given in Tables 1 and 3.

The solvation effect on the first **1**→**2-TS**→**3** cycloaddition step is very limited in all the solvents studied; the activation energy becomes lower by about 1 kcal mol^{-1} and the exothermicity of ring allene formation increases by about 3 kcal mol^{-1}. Varying the polarity of the medium does not significantly change the solvent effect in this stage of the reaction.

Comparison of gas-phase and solvation ΔG surfaces of ring allene **3** conversion shows the largest difference in the first 1,2-hydrogen shift of Pathway II (**3**→**7-TS**→**8**) and **5**→**6-TS**→**10** isomerization in Pathway I. For the intermolecular reaction the activation barrier of the 1,2-hydrogen shift changes from 31.1 kcal/mol^{-1} in the gas phase to 28.6 kcal mol^{-1} in toluene and, finally, decreases to 21.6 kcal mol^{-1} in water. The endothermicity of carbene **8** formation from allene **3** also decreases from 16.3 kcal mol^{-1} in the gas phase to 15.1 kcal mol^{-1} in toluene and 12.6 kcal mol^{-1} in water. The isomerization activation barrier for **5** changes in the same manner, decreasing by about 7 kcal mol^{-1}. The entire chemical transformation to the final aromatic product becomes more favorable by 5 kcal mol^{-1} upon changing from the gas phase to a water environment.

It should be noted in conclusion that solvation by toluene or chloroform does not lead to significant changes in the energy surface of the reaction; a valuable solvent effect may be effected from a more polar surrounding such as DMSO or water. Not surprisingly, the present calculations did not find a substantial solvent effect on the rate-determining [4 + 2] cycloaddition stage of the reaction. The result is in good agreement with literature data.[18,20] Therefore one would not expect a large dependence of reaction rate on the medium, although some steps may benefit from solvation in polar surroundings owing to lowered activation barriers and increased exothermicity.

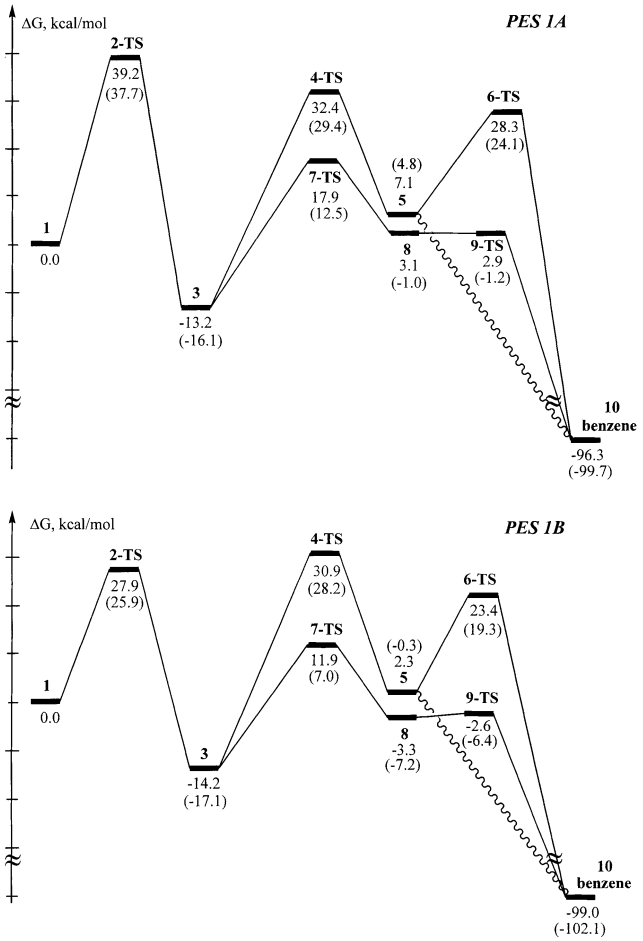

Figure 3. Top:PES 1A, intermolecular model reaction of acetylene and enyne. Bottom: PES 1B, intramolecular reaction. Both calculated at the MP2/6–31G* level; PCM (toluene) MP2/6–31G* values are given in parentheses

DISCUSSION

The above results represent the first computation of the total potential energy surface of the [4 + 2] enyne cycloaddition reaction mechanism. The unique feature of the intermolecular potential energy surface studied is that it interconnects very interesting intermediate species **3, 8** and **5**, which have been proposed in different conversion and isomerization reactions.[2,6,7,9,11,12,39] In

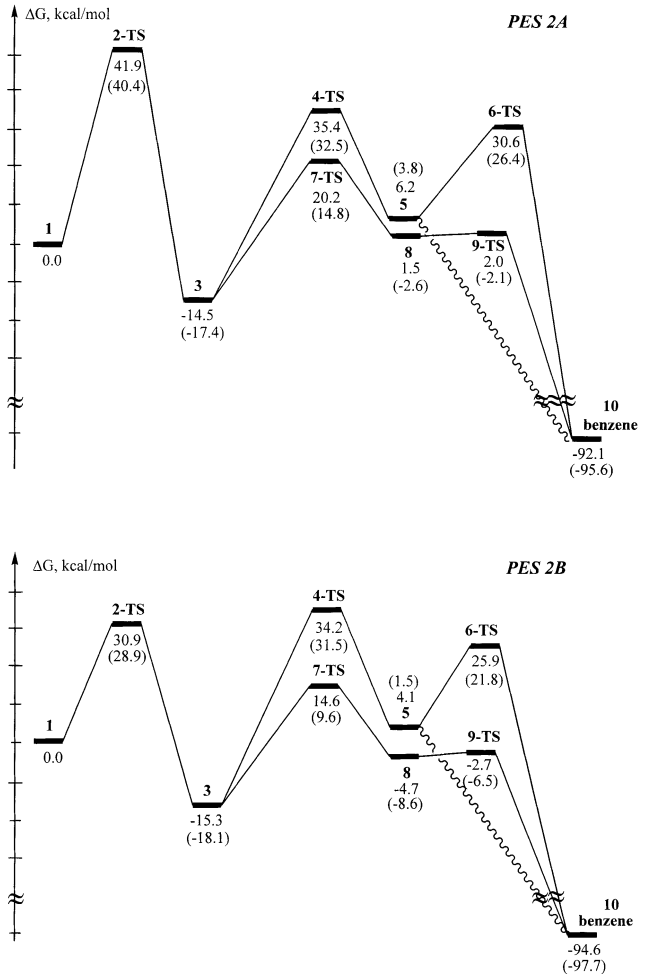

Figure 4. Top: PES 2A, intermolecular model reaction of acetylene and enyne. Bottom: PES 2B,intramolecular reaction. MP4(SDTQ)/6–31G* energy and MP2/6–31G* calculated thermal correction to Gibbs free energy; PCM (toluene) MP2/6–31G* solvent effect corrected values are given in parentheses

addition, the potential energy surface for substituted bicyclic derivatives (intramolecular reaction) is reported for the first time. To the best of our knowledge, the present investigation represents a new route to the *cis,cis,trans*-1,3,5-cyclohexatriene referred as 'Möbius benzene' starting from the parent cyclic six-membered allene (1,2,4-cyclohexatriene).

The following major points are selected for discussion.

1. High-level electron correlation calculations have shown that MP2 may underestimate activation barriers in the studied system by 2–6 kcal mol^{-1}. MP3 and MP4(SDQ) energies also may not be accurate enough and full MP4(SDTQ) calculations should be used instead. The same is true for the CCSD level, while the CCSD(T) energy surface agrees well with the MP4(SDTQ) calculated one. Nevertheless, no dramatic MP2 failures were found in the system studied and the method can be accepted as reliable quantitatively.

PCM calculations do not show a significant dependence of the [4 + 2] cycloaddition stage rate on the type of media in agreement with expectations for hydrocarbon reactions. The energy parameters of the cycloaddition stage are almost unaffected on changing from the gas phase to a polar solvent such as water. The largest solvent effect of the order of 7–10 kcal mol^{-1} was found for the first 1,2-hydrogen shift of Pathway II and the last isomerization step of Pathway I.

Finally, the best potential free energy surfaces for intermolecular (PES 2A) and intramolecular (PES 2B) reactions can be constructed using MP4(SDTQ) energies, thermal correction to Gibbs free energy calculated at the MP2 level and accounting for the solvent effect within the PCM approach (Fig. 4). We believe that the surfaces represent one of the most accurate descriptions of the system under investigation.

2. Both intermolecular and intramolecular reactions proceed through similar transition states forming a six-membered allene as an intermediate. However, the activation free energies for the reactions differ dramatically, being 11.3 kcal mol^{-1} smaller for the intermolecular cycloaddition. This is a well known advantage of intramolecular over intermolecular reactions and can be attributed to lowered activation entropy in the former case. As shown in Table 1, for the intermolecular process the deviation in MP2/6-31G* activation energy ($\Delta E^{\neq}$) and MP2/6-31G* activation free energy ($\Delta G^{\neq}$) for the first step is 13.5 kcal mol^{-1}, the same difference for the intermolecular reaction is only 3.6 kcal mol^{-1}. Entropy also significantly changes the exothermicity of ring allene formation, which is $\Delta E = -31.6$ kcal mol^{-1} and -21.2 kcal mol^{-1} for intermolecular and intramolecular cycloaddition respectively, at the MP2/6–31G* surface. The former value is close to the -29.7 kcal mol^{-1} predicted using the additivity method.[1] On the free energy MP2/6–31G* surface both reactions have similar exothermicity ($\Delta G = -13.2$ and -14.2 kcal mol^{-1}), consistent with the -13.4 kcal mol^{-1} exothermicity calculated with *ab initio* theory.[2]

The calculated relatively high activation barriers agree very well with experimental observations,[1,3] which indicate a non-catalyzed reaction in the temperature range 100–250 °C and very slow reaction at 40 °C.

From the above discussion, two important considerations deserve special note. First, is the necessity for Gibbs free energy calculations to construct the total potential energy surface of the entire reaction. Next, although an intermolecular cycloaddition reaction correctly reproduces qualitative trends, it should not be used as a simplified model for experimentally developed intramolecular synthetic applications. Owing to the large activation energy and transition state geometry differences, an explicit system treatment is much more reliable.

On the MP4(SDTQ) energy surface (PES 2A) the intermolecular cycloaddition step has $\Delta G^{\neq} = 41.9$ kcal mol^{-1} and $\Delta G = -14.5$ kcal mol^{-1} (40.4 and -17.4 kcal

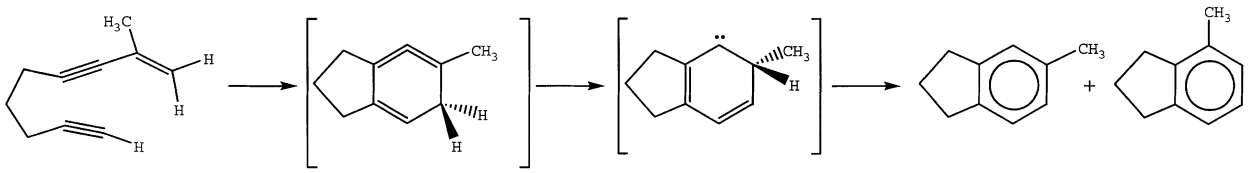

11 12 13 14 15

Scheme 4. Experimental cycloaddition reaction 2

mol^{-1} in toluene surrounding); corresponding values for the intramolecular (PES 2B) reaction are $\Delta G^{\neq} = 30.9$ kcal mol^{-1} and $\Delta G = -15.3$ kcal mol^{-1} (28.9 and -18.1 kcal mol^{-1} on the PCM-toluene surface).

3. Detailed examination of the possible conversion of ring allene **3** to aromatic system **10** reveals two alternative pathways; 1,3-hydrogen shift followed by isomerization (Pathway I) and two subsequent 1,2-hydrogen shifts (Pathway II). The activation barrier of the 1,3-hydrogen shift (**3** $\rightarrow$ **4 TS**) is in both cases (inter- and intramolecular processes) higher than that for the first 1,2-hydrogen shift (**3** $\rightarrow$ **7 TS**). On the potential energy surface of the intramolecular reaction **4-TS** is even higher in energy than the cycloaddition step transition state **2-TS**. Pathway II is dramatically less demanding energetically and most likely is the one that takes place in the real system.

These results explain the difficulties in isolating or observing six-membered allene intermediates in the reactions, since 1,2-hydrogen shifts require mush smaller activation energies than the first cycloaddition steps. According to the calculations, the [4 + 2] cycloaddition is the rate-determining stage of the enyne to aromatic hydrocarbon conversion.

The first 1,2-hydrogen shift of Pathway II on the MP4(SDTQ) energy surface (PES 2A) intermolecular cycloaddition step has $\Delta G^{\neq} = 34.7$ kcal mol^{-1} and $\Delta G = 16.0$ kcal mol^{-1} (32.2 and 14.8 kcal mol^{-1} on the PCM–toluene surface); corresponding values for the intramolecular reaction (PES 2B) are $\Delta G^{\neq} = 29.9$ kcal mol^{-1} and $\Delta G = 10.6$ kcal mol^{-1} (27.7 and 9.5 kcal mol^{-1} on the PCM–toluene surface).

The conclusions drawn concerning the mechanism of ring allene conversion can be confirmed with available experimental data. Thermolysis of **11** gives two bicyclic products **14** and **15**, with 58% and 17% yields, respectively (Scheme **4**). The formation of both isomers **14** and **15** was unexpected, but can be explained in terms of Pathway II. After the first 1,2-hydrogen shift a carbene intermediate **13** is formed (like **8**, but with a CH_3 group instead of an H atom at C_2 see Fig. 2). The next shift may involve either a hydrogen atom leading to **14** of a methyl group giving **15**. The calculations in the present work show a very low activation barrier for the second shift starting from carbene **8** and the process may also involve the methyl group to produce the corresponding isomer **15**. Not surprisingly, the hydrogen atom as a non-directional migrating group shifts more easily, thus resulting in a higher yield of **14**. These experimental observations were made using flash vacuum thermolysis[2].

The conversion of the ring allene through a 1,2-shift with subsequent carbene intermediate generation is also supported with other experimental findings[3].

To summarize, the present investigation reveals an appropriate ring allene conversion mechanism correct from both experimental and theoretical points of view.

4. It will be interesting to compare ring allene conversion pathways in intermolecular and intramolecular reactions, and obviously the main differences between Pathway I and Pathway II should also be outlined. The factors controlling the direction of the conversion process would include both steric and electronic contributions. Energy changes accompanying rearrangement through Pathway I reflect a high steric demand, since the formation of **4-TS** requires large skeletal angle bending. The non-planar structure of the carbon ring increases steric strain and shifts the pathway to the top of the potential energy surface. As a result, activation and reaction energy parameters for Pathway I are very similar for intermolecular and intramolecular reactions, and neither transition state geometry shows a significant difference.

In contrast to the former, 1,2-hydrogen shifts occur in the planar conformation of the carbon skeleton of the six-membered ring (**7-TS, 8** and **9-TS**) and are not much influenced by steric factors. Some stabilization effect from the second alkyl ring may be an additional source of energy gain. This makes Pathway II lower in energy than Pathway I in all cases and the former pathway is more sensitive to the presence of substituents.

Thus, the main differences between intermolecular and intramolecular reactions are lower barriers of the cycloaddition and the first 1,2-hydrogen shift stages due to the activation entropy contribution and alkyl ring stabilization effects.

Intermolecular acetylene and vinylacetylene coupling to benzene has not been recognized as a valuable experimental method, but the intramolecular reaction has shown substantial synthetic potential[1,3]. This can be explained in the light of the theoretical study performed and supports the calculations results obtained.

5. Aromatic ring **(10)** formation from the initial enyne precursor **(1)** is a highly exothermic process by 96.3 and 99.0 kcal mol^{-1} (99.7 and 102.1 kcal mol^{-1} according to PCM modeling of the toluene environment) for intermolecular and intramolecular cycloaddition reactions, respectively, on the MP2 energy surface and by 92.1 and 94.6 kcal mol^{-1} on the MP4(SDTQ) energy surface (95.6 and 97.7 kcal mol^{-1} on the PCM–toluene surface). Such high exothermicity provides the necessary driving force and renders the chemical transformation irreversible. The energy gain comes mostly from two effects: two relatively strong carbon–carbon σ-bonds are formed instead of a weak acetylenic π-bonds, and due to aromatic stabilization energy.

CONCLUSIONS

This detailed examination of the [4+2] enyne cycloaddition reaction pathway in the light of available experimental data allows the following conclusions to be drawn.

The rate-determining stage of the reaction is the first enyne + alkyne cycloaddition step. A non-planar six-membered ring allene intermediate can be converted to an aromatic system starting via either a 1,3- or a 1,2-hydrogen shift. The latter pathway has a lower activation energy and proceeds through intermediate carbene generation. The calculated energy surface provides a reliable explanation of the available experimental data.

A non-catalyzed thermal cycloaddition reaction was studied. Further investigations of the system under different reaction conditions and involving substituted substrates are the subject of ongoing work.

Supplementary material

Coordinates in *xyz* format for the optimized geometries of all structures are available at the epoc website at http://www.wiley.com/epoc.

Acknowledgements

The author thanks Dr Alex A. Granovsky for helpful comments on some PC-GAMESS features and Drs Vitaly Solkan and Georgy Zatonsky for stimulating discussions.

REFERENCES

1. Danheiser RL, Gould AE, de la Pradilla RF, Helgason AL *J. Org. Chem*, 1994; **59**: 5514.
2. Burrel RC, Daoust KJ, Bradley AZ, DiRico KJ, Johnson RP *J. Am. Chem. Soc* 1996; **118**: 4218.
3. Wills MSB, Danheiser RL *J. Am. Chem. Soc.* 1998; **120**: 9378.
4. Gilchrist TL *J. Chem. Soc. Perkin Trans. 1* 1999; 2849.
5. Christl M, Braun M, Müller G *Angew. Chem. Int. Ed. Engl.* 1992; **31**: 473.
6. Johnson RP *Chem. Rev.* 1989; **89**: 1111.
7. Janoschek R *Angew. Chem. Int. Ed. Engl.*, 1992; **31**: 476.
8. Hopf H, Berger H, Zimmermann G, Nüchter U, Jones PG, Dix I *Angew. Chem. Int. Ed. Engl.* 1997; **36**: 1187.
9. Roth WR, Hopf H, Horn C *Chem. Ber.* 1994; **127**: 1765.
10. Li Z, Rogers DW, McLafferty FJ, Mandziuk M, Podosenin AV *J. Phys. Chem. A*1999; **103**: 426.
11. Merz KM, Scott LT *J. Chem. Soc. Chem. Commun.* 1993; 412.
12. Bettinger HF, Schreiner PR, Schaefer HF, Schleyer PvR *J. Am. Chem. Soc.*, 1998; **120**: 5741.
13. Møller C, Plesset MS *Phys. Rev.* 1934; **46**: 618.
14. Frisch MJ, Head-Gordon M, Pople JA *Chem. Phys. Lett.* 1990; **166**: 275.
15. Ditchfield R, Hehre WJ, Pople JA *J.Chem. Phys.* 1971; **54**: 724.
16. Krishnan R, Binkley JS, Seeger R, Pople JA *J. Chem. Phys.* 1980; **72**: 650.
17. Gonzales C, Schlegel HB *J. Chem. Phys.* 1989; **90**: 2154.
18. Tomasi J, Persico M *Chem. Rev.* 1994; **94**: 2027.
19. Amovilli C, Barone V, Cammi R, Cances E, Cossi M, Mennucci B, Pomelli CS *Adv. Quantum. Chem.* 1998; **32**: 227.
20. Cramer CJ, Truhlar DG *Chem. Rev.* 1999; **99**: 2161.
21. Barone V, Cossi M, Tomasi J *J. Chem. Phys.* 1997; **107**: 3210.
22. *CRC Handbook of Chemistry and Physics* (77th edn). Lide DR (ed) CRC Press: Boca Raton, FL, 1996.
23. Pople JA, Seeger R, Krishnan R *Int. J. Quantum. Chem. Symp.* 1977; **11**: 149.
24. Hehre WJ, Radom L, Schlaer PvR, Pople JA *Ab Initio Molecular Orbital Theory.*Wiley: New York, 1986.
25. Pulay P, Saebo S, Meyer W *J. Chem. Phys.* 1984; **81**: 1901.
26. Saebo S, Pulay P *J. Chem. Phys.* 1987; **86**: 914.
27. Krishnan R, Frisch MJ, Pople JA *J. Chem. Phys.* 1980; **72**: 4244.
28. Pople JA, Head-Gordon M, Raghavachari K *J. Chem. Phys.* 1987; **87**: 5968.
29. Bartlett RJ, Purvis GD III *Int. J. Quantum. Chem.* 1978; **14**: 561.
30. Bartlett RJ, Purvis GD III *Phys. Scr.* 1980; **21**: 255.
31. Raghavachari K, Trucks GW, Pople JA, Head-Gordon M *Chem. Phys. Lett.* 1989, **157**: 479.
32. Granovsky AA PC-GAMESS version 5.5 Moscow State University: Moscow, 1999.
33. Schmidt MW, Baldridge KK, Boatz JA, Elbert ST, Gordon MS, Jensen JJ, Koseki S, Matsunaga N, Nguyen KA, Su S, Windus TL, Dupuis M, Montgomery JA *J. Comput. Chem.* 1993; **14**: 1347.
34. Frisch MJ, Trucks GW, Schlegel HB, Scuseria GE, Robb MA, Cheeseman JR, Zakrzewski VG, Montgomery, JA Jr, Stratmann RE, Burant JC, Dapprich S, Millam JM, Daniels AD, Kudin KN, Strain MC, Farkas O, Tomasi J, Barone V, Cossi M, Cammi R, Mennucci B, Pomelli C, Adamo C, Clifford S, Ochterski J, Peterson GA, Ayala PY, Cui Q, Morokuma K, Malick DK, Rabuck AD, Raghavachari K, Foresman JB, Cioslowski J, Ortiz JV, Stefanov BB, Liu G, Liashenko A, Piskorz P Komaromi I Gomperts R, Martin RL, Fox DJ, Keith T, Al-Laham MA, Peng CY, Nanayakkara A, Gonzalez C, Challancombe M, Gill PMW, Johnson B, Chen W, Wong MW, Andres JL, Gonzalez C, Head-Gordon M, Replogle ES, Pople JA Gaussian 98, Revision A.7 Gaussian:Pittsburgh, PA, 1998.
35. Schaftenaar G, Noordik JH *J. Comput.-Aided Mol. Des.* 2000; **14**: 123.
36. Johnson RP, Daoust KJ *J. Am. Chem. Soc.* 1996; **118**: 7381.
37. Cramer CJ, Truhlar DG, Falvey DE *J. Am. Chem. Soc.* 1997; **119**: 12338.
38. Nickon A *Acc. Chem. Res.* 1993; **26**: 84.
39. Sulzbach HM, Platz MS, Schaefer HF, Hadad CM *J. Am. Chem. Soc.* 1997; **119**: 5682.
40. Hehre WJ, Ditchfield R, Pople JA *J. Chem. Phys.* 1972; **56**: 2257.
41. Krishnan R, Pople JA *Int. J. Quantum. Chem.* 1978; **14**: 91.